ADAM10 and γ-Secretase Regulate Sensory Regeneration in the Avian Vestibular Organs

Mark E. Warchol[1*], Jennifer Stone[2*], Matthew Barton[1], Jeffrey Ku[3], Rose Veile[1,3], Nicolas Daudet[4], Michael Lovett[3,5]

[1]Department of Otolaryngology, Washington University School of Medicine, St. Louis, MO, 63110

[2]The Virginia Merrill Bloedel Hearing Research Center and Department of Otolaryngology—Head and Neck Surgery, University of Washington School of Medicine, Seattle, WA 98195

[3]Department of Genetics, Washington University School of Medicine, St. Louis, MO, 63110

[4]Center for Auditory Research, University College London, London

[5]NHLI, Imperial College, London

*M.E.W. and J.S. contributed equally to this research

Corresponding Author:
Mark E. Warchol
Department of Otolaryngology
Box 8115
Washington University School of Medicine
660 South Euclid Ave
St Louis MO 63110

Word counts:
Abstract: 258
Introduction: 647
Methods: 1,312
Results: 2,833
Discussion: 2,002
35 pages of text
8 figures
3 tables

Supported by grants R01 DC006283 (ME Warchol), T32 DC000022 (JF Piccirillo), P30 DC04665 (RA Chole), R01 DC003696 (JSS), P30 DC04661 (EW Rubel), and RC1DC010677 (ML). For experiments conducted at the University of Washington, we acknowledge Jialin Shang for culture preparation and maintenance and Glen MacDonald for assistance with digital imaging. Finally, we dedicate this manuscript to the memory of our colleague and coauthor Matthew Barton, who passed away in January, 2017.

Abstract

The loss of sensory hair cells from the inner ear is a leading cause of hearing and balance disorders. The mammalian ear has a very limited ability to replace lost hair cells, but the inner ears of non-mammalian vertebrates can spontaneously regenerate hair cells after injury. Prior studies have shown that replacement hair cells are derived from epithelial supporting cells and that the differentiation of new hair cells is regulated by the Notch signaling pathway. The present study examined molecular influences on regeneration in the avian utricle, which has a particularly robust regenerative ability. Chicken utricles were placed in organotypic culture and hair cells were lesioned by application of the ototoxic antibiotic streptomycin. Cultures were then allowed to regenerate *in vitro* for seven days. Some specimens were treated with small molecule inhibitors of γ-secretase or ADAM10, proteases which are essential for transmission of Notch signaling. As expected, treatment with both inhibitors led to increased numbers of replacement hair cells. However, we also found that inhibition of both proteases resulted in increased regenerative proliferation. Subsequent experiments showed that inhibition of γ-secretase or ADAM10 could also trigger proliferation in undamaged utricles. To better understand these phenomena, we used RNA-Seq profiling to characterize changes in gene expression following γ-secretase inhibition. We observed expression patterns that were consistent with Notch pathway inhibition, but we also found that the utricular sensory epithelium contains numerous γ-secretase substrates that might regulate cell cycle entry and possibly supporting cell-to-hair cell conversion. Together, our data suggest multiple roles for γ-secretase and ADAM10 in vestibular hair cell regeneration.

Introduction

The hair cells of vestibular organs detect linear and rotational head movements, providing sensory information that is essential for normal postural and visual reflexes. Most vestibular hair cells are produced during embryonic development, but they can be lost later in life as a consequence of ototoxicity or as part of normal aging (humans: Merchant et al., 2000; Rauch et al., 2001; Lopez et al., 2005; mice: Park et al., 1987). Mature mammals possess a limited ability to replace hair cells after injury (e.g., Forge et al., 1993; 1998; Kawamoto et al., 2009; Lin et al., 2011; Golub et al., 2012), and their loss often results in permanent deficits in balance and equilibrium. In contrast, the vestibular organs of non-mammalian vertebrates can quickly regenerate lost hair cells, leading to restoration of sensory function (reviewed in Warchol, 2011). Such regenerated hair cells are derived from non-sensory cells called supporting cells, which reside alongside hair cells within the vestibular sensory epithelia. Supporting cells can form new hair cells, either by cell division or by direct phenotypic conversion (reviewed in Stone and Cotanche, 2007). Identification of the signals that control hair cell regeneration in non-mammalian vertebrates is an important step in the development of strategies to promote restoration of balance function in the human inner ear after injury or age-related pathologies.

During otic development, differentiation of sensory hair cells is modulated by the Notch pathway (reviewed in Kelley, 2006). Notch is a membrane-bound receptor that is activated by ligands expressed on adjacent cells (Kopan and Ilagan, 2009). During the development of the inner ear, nascent hair cells express Notch ligands that interact with receptors on neighboring progenitor and supporting cells, preventing those cells from adopting a hair cell fate. Transmission of a Notch signal requires two sequential proteolytic events. Following interaction with a Notch ligand (i.e., Delta or Jagged), the Notch receptor is first cleaved near its extracellular surface via the metalloprotease ADAM10 (van Tetering et al., 2009). Next, the intracellular portion of the receptor is cleaved by γ-secretase, permitting the Notch intracellular domain

(NICD) to translocate to the nucleus and regulate gene expression (e.g., Kopan, 2012).

Genetic disruption of Notch signaling in the developing inner ear leads to the production of supernumerary hair cells (e.g., Haddon et al., 1998; Lanford et al., 1999; Yamamoto et al., 2006). Inhibition of γ-secretase signaling has a similar effect during inner ear development (e.g., Takebayashi et al., 2007; Hayashi et al., 2008; Doetzlhofer et al., 2009), and it significantly augments hair cell regeneration in the auditory organ (basilar papilla) of mature birds (Stone and Rubel, 1999; Daudet et al., 2009), the neuromasts of larval fish (Ma et al., 2008; Romero-Carvajal et al., 2015), and the vestibular organs of adult mice (Lin et al., 2011; Slowik et al., 2013). However, these studies left some questions unanswered. First, it is not clear that Notch is the critical or sole target of y-secretase inhibition; other γ-secretase substrates besides Notch may also modulate hair cell regeneration. Further, effects of γ-secretase inhibitors in avian vestibular hair cell regeneration have not been tested.

The present study examined the role of γ-secretase or ADAM10 in the mature chicken utricle, a vestibular organ that detects linear acceleration. During regeneration, we found that inhibition of either protease resulted in a dramatic increase in hair cell differentiation, indicating that Notch-dependent lateral inhibition regulates hair cell fate decisions during regeneration. Inhibition of γ-secretase or ADAM10 after hair cell destruction also increased the proliferation of supporting cells, pointing to an important role for these enzymes in regulating cell cycle entry. Moreover, inhibition of either enzyme evoked a robust proliferative response in the *undamaged* utricle, suggesting that activation of both γ-secretase and ADAM10 is necessary for maintaining supporting cells in a quiescent state. Although such regulation is likely mediated by Notch signaling, transcriptional profiling by RNA sequencing identified other substrates that may also influence cell cycle entry.

Materials and Methods

Animals

Experiments conducted at Washington University (St. Louis MO) used White Leghorn chickens. Fertile eggs were obtained from Charles River (Franklin, CT), and incubated for 20-21 days (d) at 37^{o}C in facilities managed by the Washington University Department of Comparative Medicine. Hatchling chicks were then kept for 10-20 d in heated brooders. Experiments conducted at the University of Washington (Seattle) also utilized White Leghorn chickens, which were hatched from fertile eggs (Featherland Farms, Coburg, OR) and maintained in vivarium facilities at the University of Washington. Post-hatch chickens were maintained in heater brooders with ample food and water until the end of each experiment. All experimental protocols involving animals were approved by the Washington University Institutional Animal Studies Committee or the University of Washington Animal Care Committee, and conformed to the National Institutes of Health animal use guidelines.

Organ culture techniques

Most experiments utilized organotypic cultures of the chicken utricle, which were prepared according to previously published protocols (e.g., Warchol and Montcouquiol, 2010). Briefly, chickens (10-20 d post-hatch) were euthanized via CO_2 inhalation and quickly decapitated. The lower jaw and skin were removed, and heads were immersed in 70% ethanol for ~5-10 minutes (min), in order to kill surface pathogens. The middle ear space was opened and the membranous labyrinth was exposed. At this point, a small portion of the temporal bone (containing the utricle) was removed and transferred to chilled Medium-199 (with Hank's salts and HEPES buffer, Invitrogen). Utricles were carefully isolated from their temporal bone substrates, and the otoconia and otolithic membranes were removed. The remaining sensory organs were transferred to culture wells (MatTek) that contained 100 µl of medium (Medium-199 supplemented with Earle's salts, 2,200 mg/L sodium bicarbonate, 0.69 mM L-glutamine, 25 mM

HEPES, and 1% Fetal Bovine Serum (FBS; Invitrogen). All cultured specimens were incubated at 37˚C in a humidified 5% CO_2/95% air environment. Some cultures were initially treated for 24 hour (hr) in 100 µM or 1 mM streptomycin sulfate (Sigma-Aldrich), and were then rinsed 3x in fresh medium and maintained in streptomycin-free medium for an additional 2d or 7d.

Small molecule inhibition of γ-secretase and ADAM10

Most experiments involved the inhibition of either γ-secretase or ADAM10, which are proteases required for transmission of Notch signaling between adjoining cells. Inhibition of γ-secretase was accomplished by addition of N-[N-(3,5-Difluorophenacetyl)-L-alanyl]-S-phenylglycine t-butyl ester (DAPT, Sigma-Aldrich) to the culture medium. Specimens were maintained in 10 µM DAPT for either 48 hr or for 7 d. Medium in DAPT-treated cultures was changed at 24 hr intervals. Other cultures were treated with GM6001 (20 µM, EMD Millipore, a general metalloprotease inhibitor), TAPI-2 (50 µM, EMD Millipore, an inhibitor of ADAM-family proteases) or GI254023X (10 µM, Tocris Bioscience, a specific inhibitor of ADAM10). Medium in metalloprotease-inhibited cultures was changed at 48 hr intervals. All protease inhibitors were prepared as 1,000x stock solutions (in DMSO) and stored at -20^{o}C. Control cultures contained 0.1% DMSO. Finally, some cultures contained bromodeoxyuridine (BrdU, 3 µg/ml) for the final 4 hr *in vitro*, in order to label proliferating cells.

Preparation of isolated epithelial cultures

Cultures of isolated sensory epithelia from the chicken utricle were prepared according to methods modified from those outlined in Warchol (2002). Briefly, utricles were removed from chicks and dissected, as described above. Sensory organs were then incubated for 60 min in 500 µg/ml thermolysin (Sigma-Aldrich) at 37^{o}C, and transferred to chilled Medium-199 (with Hanks salts and HEPES). Using a fine needle, the sensory epithelia were carefully isolated from the underlying stromal tissue and placed (lumenal side-up) on laminin-coated glass surfaces of culture wells (MatTek) that contained 30 µl of Medium-199 (with

Earle's salts, as above), supplemented with 10% FBS. Specimens were incubated at 37°C and additional medium was added (in 10 µl aliquots) every 2 hr, for a final volume of 50 µl. Cultures were maintained in this medium for 48 hr, in order to allow time for the epithelia to adhere to the laminin substrates. The medium was then replaced with 100 µl of Medium-199 (with Earles salts and 1% FBS), that also contained either 10 µM DAPT or 0.1% DMSO. Cultures were incubated in these media for 24 hr. Some cultures received BrdU for the final 4 hr *in vitro*, and were used to assess cell proliferation (e.g., Fig. 6). Other cultures were used for RNA-Seq profiling (see Results).

Immunocytochemical methods

All specimens were fixed for 30 min with 4% paraformaldehyde in 0.1 M phosphate buffer (pH=7.4), and then rinsed 5x with 0.01M phosphate buffered saline (PBS; Sigma-Aldrich). Nonspecific antibody binding was blocked by treatment for 2 hr in 5% normal horse serum in PBS, with 0.2% Triton X-100. Specimens were treated for 16-20 hr at room temperature with one of the following antibodies: rabbit polyclonal antiserum directed against atonal homolog 1, or ATOH1 (1:300, from Jane Johnson, University of Texas Southwestern Medical Center); rabbit polyclonal antiserum directed against myosin VIIa (1:500, #25-6790, Proteus Biosciences); or mouse monoclonal directed against ß tectorin precursor (1:1000; from Guy Richardson, University of Sussex, UK). All primary antibodies were dissolved in PBS with 2% NHS and 0.2% Triton X-100. Specimens were then thoroughly rinsed and treated for 2 h at room temperature with Alexa-conjugated secondary antibodies (Invitrogen). Some specimens were also labeled with Alexa-488-conjugated phalloidin (Invitrogen) to detect filamentous actin or 4',6-diamidino-2-phenylindole (DAPI) to detect DNA. After labeling, specimens were placed on microscope slides in a drop of glycerol:PBS (9:1) or Fluoromount and cover-slipped.

To detect BrdU, specimens were fixed as described and then treated for 30 min with 2N HCl. Specimens were maintained for 16-20 hr at room temperature in monoclonal anti-BrdU (either mouse-anti-BrdU, BD Biolsciences, 1:50 or

SeraLabs rat-anti-BrdU, 1:500) dissolved in PBS with 10% NHS and 1.0% Triton X-100. Specimens were treated with secondary antibodies conjugated to an Alexa dye (Invitrogen), labeled with DAPI, and coverslipped as described above.

Quantification from organotypic cultures

Specimens were imaged on a Zeiss LSM700 confocal microscope, and maximum intensity projections were constructed from stored image stacks using Volocity software (PerkinElmer). Cell quantification was conducted directly from these full depth projections. Cell proliferation was assessed by counting BrdU-labeled cell nuclei within six 100x100 μm regions of the sensory epithelium. The sampled regions were located in the extrastriolar portion of the sensory epithelium, and were approximately evenly spaced and distributed along the anterior-posterior axis. Hair cell densities were quantified from confocal images of myosin VIIa-labeled cells, using a similar sampling scheme.

RNA-Seq preparation and analyses

Isolated sensory epithelia were treated for 24 hr in 10 μM DAPT or 0.1% DMSO. Samples were harvested by replacing the medium with 100 μl of Trizol (Life Technologies), triturating 10x, and processed using Illumina TrueSeq preparation kits, as previously described (Ku et al 2014). In brief, mRNA was selected by oligo-dT magnetic beads from 1 μg of total RNA and fragmented. First-strand cDNA was generated using random primers. Second-strand synthesis, end repair, addition of a single A base, adaptor ligation and amplification were then performed. Each library was sequenced using the Illumina HiSeq 2000. In all cases, biological replicate samples from pure sensory epithelia were analyzed. Each biological sample consisted of 8 pooled sensory epithelia that were treated with either 10 μM DAPT or 0.1% DMSO. Raw reads in FASTQ format were aligned to the Ensembl *Gallus gallus* reference genome (WUGSC2.1 E66) using Tophat v1.4.0 (Trapnell et al., 2009). The output .bam file was processed by Partek Genomics Suite v6.6 (Partek Inc., St. Louis, MO) to assemble reads into transcripts and estimate their abundances. A gene model data set combining Ensembl and NCBI annotations was used to generate RPKM

(Reads Per Kilobase of exon per Million fragments mapped) for known genes and potential novel transcripts. Statistical significance levels were calculated by one-way analysis of variance (ANOVA). Reads mapped to different isoforms of a given gene were combined together for analysis. All sequence data and annotations have been submitted to NCBI GEO and are available online.

Results

Inhibition of γ-secretase following vestibular hair cell damage leads to increased numbers of regenerated hair cells

Prior data indicate that inhibition of γ-secretase enhances hair cell regeneration in the auditory sensory organ (basilar papillae) of birds (Daudet et al., 2009; Lewis et al., 2012). Our initial experiments focused on characterizing the effects of γ-secretase inhibition on hair cell regeneration in the chick utricle, a vestibular sensory organ that contains ~29,000 hair cells and detects linear acceleration (Goodyear et al, 2009). The sensory region of the utricle also contains a specialized region called the striola, which is located near the lateral edge of the epithelium and possesses several unique morphological features. In the center of the striola, hair cell orientation undergoes an abrupt 180^{o} shift; this region is known as the striolar reversal zone. The regions of the sensory epithelium that are outside of the striola are known as the extrastriolar regions (e.g., Jørgensen, 1989).

To assess effects of γ-secretase inhibition, whole utricles (n=20) were explanted and cultured for 24 hr with 1 mM streptomycin, which kills most hair cells (Warchol and Montcouquiol, 2010). Specimens were then thoroughly rinsed and maintained *in vitro* for an additional 7 d. During this recovery period, some utricles (n=10) were treated with 10 μM DAPT (N-[N-(3,5-Difluorophenacetyl-L-Aalanyl)]-S-phenylglycine t-butyl ester), a specific inhibitor of γ-secretase. The remaining specimens were treated with 0.1% DMSO (the vehicle for DAPT) and served as controls. After fixation, utricles were immunolabeled for myosin VIIa (to identify hair cells) and stained with phalloidin (to label actin filaments).

Treatment with DAPT resulted in striking increases in the numbers of myosin VIIa-labeled hair cells in both the striolar region and the extrastriolar regions (Fig. 1). Precise measurements of hair cell numbers or hair cell-to-supporting cell ratios in DAPT-treated specimens were not feasible, because myosin VIIa-labeled cells were often tightly packed together and individual cell borders were not discernible.

Inhibition of ADAM metalloproteases also increases hair cell regeneration in the damaged utricle

The finding of increased hair cell numbers in response to γ-secretase inhibition is consistent with the hypothesis that Notch signaling inhibits hair cell differentiation during regeneration. However, γ-secretase has over 80 identified substrates (e.g., Haapasalo and Kovacs, 2011), so it is likely that Notch was not the only pathway to have been affected by DAPT treatment. The transmission of a Notch signal between adjoining cells requires two proteolytic cleavages of the Notch receptor: the first cleavage is extracellular and mediated by the ADAM 10 metalloprotease, while the second cleavage is intracellular and mediated by γ-secretase (Kopan and Ilagen, 2009). Thus, if Notch signaling regulates the differentiation of regenerating hair cells, then inhibition of ADAM10 should also result in an overproduction of hair cells, similar to that observed after inhibition of γ-secretase. To test this prediction, we treated cultured utricles (n=10) for 24 hr with 1 mM streptomycin and then allowed them to recover for 7 d in medium that contained 10 μM GI254023X, a specific inhibitor of ADAM10 (e.g., Hundhausen et al., 2003). Control cultures (n=10) were maintained in parallel, but were treated with 0.1% DMSO (the vehicle for GI254023X). Following fixation and immunoprocessing, we observed increased numbers of hair cells in the striolar and extrastriolar regions of utricles that were treated with GI254023X, compared to the DMSO-treated controls (Fig. 1). This finding confirms that inhibition of either γ-secretase or ADAM10 (proteases that are essential for Notch receptor processing) leads to increased hair cell differentiation during regeneration after damage.

Inhibition of γ-secretase or ADAM10 also increases proliferation of hair cell progenitors following damage

Many replacement hair cells in the damaged avian ear are produced via the proliferation of supporting cells (reviewed in Stone and Cotanche, 2007; Warchol, 2011). Given that inhibition of γ-secretase led to increased hair cell regeneration, we next examined whether γ-secretase inhibition also caused an increase in supporting cell proliferation. Chicken utricles (n=16) were cultured for 24 hr with 1 mM streptomycin. All specimens were then rinsed 3x with fresh medium and incubated for an additional 48 hr in medium that contained either 10 μM DAPT (n=8 utricles) or 0.1% DMSO (n=8 utricles). Proliferating cells were labeled via the addition of bromodeoxyuridine (BrdU) to media for the final 4 hr *in vitro*. Quantification of BrdU-labeled cells indicated that DAPT treatment caused a ~3x increase in supporting cell division throughout most of the sensory epithelium (Fig. 2). Nearly identical results were obtained after inhibition of ADAM10 in the regenerating utricle. In those experiments, utricles were treated for 24 hr with 1 mM streptomycin, followed by incubation for 48 hr in 10 μM GI254023X (a specific inhibitor of ADAM10) or 0.1% DMSO (controls). Cultures also received BrdU for the final 4 hr *in vitro*. Specimens treated with GI254023X contained 97.4±45.1 (mean ± standard deviation) BrdU-labeled cells/10,000 μm^2, while controls contained 36.4±12.2 BrdU-labeled cells/10,000 μm^2 (n=6 utricles/treatment group; $p<0.02$).

Inhibition of γ-secretase causes cell cycle entry in the absence of ototoxic damage

Hair cells in the avian utricle normally undergo a slow turnover process, and a small degree of supporting cell proliferation is observed in the undamaged sensory epithelium (Jørgensen and Mathiesen, 1988; Roberson et al., 1992; Kil et al., 1997; Stone et al., 1999). Having established that inhibition of γ-secretase causes a significant increase in supporting cell division during regeneration, we next tested whether it could also increase cell cycle entry in the uninjured utricle.

Utricles were placed in organotypic culture and treated for 48 hr with either 10 μM DAPT or 0.1% DMSO (controls). BrdU was added to the media for the final 4 hr *in vitro*. High levels of proliferation were observed in DAPT-treated utricles, but not in untreated controls (Fig. 3A, B). Quantification of BrdU-labeled cells in the extrastriolar regions of DAPT-treated utricles indicated that inhibition of γ-secretase increased supporting cell proliferation by ~20x, compared to DMSO-treated controls (DAPT-treated utricles: 50.0±40.8 BrdU-labeled cells/10,000 μm^2; control utricles: 2.1±2.8 BrdU-labeled cells/10,000 μm^2; $p<0.001$). Additional experiments revealed that this proliferative effect was dose dependent, and a moderate increase in proliferation was observed after treatment with 1 μM DAPT (relative to untreated controls; Fig. 3C). Finally, the failure of BrdU-positive cells to double-label with antibodies against myosin VIIa (a known hair cell marker) indicated that the proliferating cells were supporting cells (Fig. 3D).

Inhibition of ADAM-family metalloproteases also evokes supporting cell proliferation in undamaged utricles

The observed effects of γ-secretase inhibition suggest a novel role for Notch activity in preventing supporting cell division in normal chicken utricles. As noted above, signaling via the Notch pathway can also be blocked by inhibition of ADAM metalloproteases, so we next characterized the effects of three metalloprotease inhibitors on supporting cell proliferation in uninjured utricles. Cultured utricles were treated for 48 hr with either: GM6001 (20 μM, a broad spectrum metalloprotease inhibitor), TAPI-2 (50 μM, an inhibitor specific for ADAM-family metalloproteases), or GI254023X (10 μM, specific inhibitor for ADAM10). Control cultures received 0.1% DMSO. Proliferating cells were labeled by the addition of BrdU to culture media for the final 4 hr *in vitro*. In all cases, we found that metalloprotease inhibition resulted in increased supporting cell proliferation, compared to DMSO controls (Fig. 4).

Supporting cell proliferation evoked by γ-secretase inhibition is not secondary to hair cell injury

In the avian utricle, the death of hair cells triggers a proliferative response in adjoining supporting cells (e.g., Weisleder and Rubel, 1993). For this reason, it is possible that the high levels of proliferation observed after treatment with DAPT or GI254023X (Figs. 3 and 4) might be a secondary consequence of hair cell injury caused by either inhibitor. In order to rule-out this possibility, we quantified hair cells in utricles that were maintained in culture for 48 hr in 0.1% DMSO (controls) or in either 10 μM DAPT or 10 μM GI254023X. We observed normal hair cell numbers and morphology in both the drug-treated and DMSO-treated specimens (Fig. 5), indicating that neither inhibitor caused direct hair cell injury. This result confirms that such proliferation is not a consequence of DAPT- or GI254023X-induced hair cell death.

Inhibition of γ-secretase evokes proliferation in isolated vestibular supporting cells

The above data suggest that Notch activity might maintain supporting cell quiescence, but the mechanism by which this occurs is unclear. In some cell types (e.g. epidermal keratinocytes - Demehri et al., 2009), Notch activity blocks epithelial cell division indirectly, by modulating signaling between the epithelium and its underlying connective tissue. In order to determine whether a similar interaction occurs in the chicken utricle, we examined the effects of Notch inhibition on cultured sensory epithelia that were isolated from their associated stromal tissue. Utricles were explanted and incubated in thermolysin to selectively cleave the attachment between cells of the sensory epithelium (supporting cells) and the basement membrane (e.g., Warchol, 2002). Whole sensory epithelia were then removed and placed in laminin-coated culture wells. Specimens were oriented such that the basal surface of the sensory epithelium was in contact with the laminin substrate. Cultures were first incubated for 72 hr, to allow for attachment of the epithelial cells to their substrates. At this point, culture media were replaced with media containing either 10 μM DAPT or 0.1% DMSO (controls), and cultures were maintained for an additional 24-48 hr. BrdU was added to all cultures for the final 4 hr *in vitro*. Quantification of BrdU-labeled

cells revealed that DAPT treatment caused a large increase in cell proliferation in these isolated epithelia ($p<0.005$; Fig. 6). Because hair cells are thought to be terminally post-mitotic, we assume that the dividing cells were supporting cells. These results were reminiscent of DAPT effects in intact cultured utricles (e.g., Fig. 3), and demonstrate that the protease-dependent signals that regulate supporting cell proliferation are confined to the sensory epithelium.

Regional variability in the responsiveness to γ-secretase inhibition

In both undamaged and ototoxin-lesioned utricles, DAPT treatment resulted in increased hair cell differentiation and supporting cell proliferation throughout the majority of the sensory epithelium (Fig. 2). However, close inspection of treated specimens revealed that DAPT had little effect on proliferation of supporting cells that were located within a narrow band running through the center of the striola region, which is the presumed site of hair cell polarity reversal (Fig. 7B,C, C'). Moreover, treatment with DAPT failed to cause either a gain in the hair cell marker myosin VIIa (Fig. 7D, D') or a loss of the supporting cell marker ß-tectorin (Fig. 7E, E') in the center of the striola. These observations suggest that cells in the central region of the utricular striola may rely on different signaling pathways to regulate both proliferation and differentiation than do cells in the remaining portions of the macula.

Changes in gene expression in response to γ-secretase inhibition

The results described above indicate that γ-secretase and ADAM10 are critical regulators of supporting cell proliferation and hair cell differentiation in the chicken utricle. Since both enzymes are required to cleave and activate the Notch receptor, our results suggest Notch activity may prevent cell cycle entry in the chicken utricle. However, γ-secretase and ADAM10 share several other substrates (in addition to Notch), so it is possible that other pathways may be involved in this process. In order to better understand the signaling pathways that underlie the observed proliferative response, we next identified those genes whose expression levels are changed by γ-secretase inhibition. Next-Generation

RNA sequencing was used to profile changes in gene expression within the utricular sensory epithelium in response to treatment with the γ-secretase inhibitor DAPT. Expression analysis was conducted on cultures of whole utricular maculae that were maintained on laminin-coated substrates (e.g., Fig. 6). Cultures were treated for 24 hr with either 10 μM DAPT or 0.1% DMSO (controls), at which point mRNA was harvested and used for RNA-Seq profiling (see Methods).

We observed significant changes ($p<0.05$ and >1.8-fold) in the expression levels of 253 genes in DAPT-treated cultures, relative to DMSO controls. [Complete list available in Supplementary Data.] We conducted a gene process enrichment analysis on this set using the online ToppGene tools (https://toppgene.cchmc.org/, data not shown). This indicated that >95 of the differentially expressed genes mapped to parts of the cell cycle process. These accounted for some of the most abundant transcripts and some of the largest changes. Ten of the differentially expressed genes mapped to Notch signaling, which was the second most significantly-affected pathway after cell cycle components. A list of the 25 identified gene transcripts that showed the largest positive fold-change is shown in Table 1. The gene whose expression was most enhanced by DAPT treatment was *Ednrb2*, an endothelin receptor that is involved in the guidance of migrating neural crest cells (Harris et al., 2008) and which also shows significant differential expression during avian hair cell regeneration (Ku et al., 2014). Enhanced expression of *Crb1* (Crumbs – a key regulator of epithelial cell polarity) was also observed. Notably, the gene whose expression was elevated to the highest abundance-level (as measured by the total number of normalized reads) was *Ccnd3* (cyclin D3), a well-characterized initiator of cell cycle entry (e.g., Sankaran et al., 2012). Other enhanced genes whose normalized expression levels were highly enriched in DAPT-treated cultures were *Mycl1* (l-myc) and *E2f1*, both of which also regulate mitosis. We also observed increases in the expression of *Mcm5* and *Mcm6*, so-called minichromosome maintenance complex components, which are involved in the

initiation of DNA replication (Chuang et al., 2012). Finally, a significant expression increase was noted for *Dll1* (Delta1), a Notch signaling ligand.

Although the hair cell-inducing transcription factor *Atoh1* was not among the 25 genes showing the largest transcriptional elevation after DAPT treatment, its expression was increased by ~3-fold. Further, in addition to increasing the numbers of regenerated hair cells, DAPT treatment also caused an increase in nuclear Atoh1 protein in sensory epithelial cells from utricles treated with streptomycin for 1 day and streptomycin-free media for another day (Fig. 8). These findings are consistent with prior studies showing that Notch activity negatively regulates Atoh1 expression (e.g., Lanford et al., 2000; Daudet et al., 2009). Some Atoh1-positive cells were mitotically active in DMSO-treated cultures, as indicated by their uptake of BrdU during the last 4 hours in culture, and their numbers appeared to increase after DAPT treatment (Fig. 8A, B). Also, at longer survival times, many of these BrdU-labeled cells differentiated as hair cells (Fig. 8C).

Conversely, a number of genes showed decreased expression after DAPT treatment. A list of the 25 genes that showed the greatest decrease in abundance in DAPT-treated samples is shown in Table 2. Many of these decreased genes provide clear evidence for a block of the Notch pathway. The most-reduced gene was *Hes5*, a principal transcriptional effector of Notch signaling. Expression of two other key Notch signaling genes – *Heyl* and *Jag1* – was also reduced. Diminished expression was also noted among a number of otherwise highly transcribed genes, such as *Tsga14*, which encodes a centrosomal protein that is implicated in autism spectrum disorders (Korvatska et al., 2011). Inhibition of γ-secretase also caused reduced expression of *Wnt7a*, a ligand that participates in both canonical and non-canonical Wnt signaling (e.g., Stenman et al., 2008) and is expressed in the cochlear duct of the developing chicken ear (Sienknecht and Fekete, 2008).

Identification of γ–secretase substrates in the utricular sensory epithelium

Our data indicate that inhibition of γ-secretase leads to significant changes in cell division, differentiation, and gene expression in the chicken utricular macula. In order to gain further insight into the molecular basis of these changes, we searched the RNA-Seq dataset obtained from utricular epithelia for known γ-secretase substrates. Haapasalo and Kovacs (2011) describe ~80 substrates for γ-secretase, of which 45 were detected (but not necessarily differentially expressed) in our dataset (>0.5 RPKM). A list of the 25 detectable γ-secretase substrates that showed the highest abundance is shown in Table 3. The most highly expressed γ-secretase target genes were the amyloid precursor protein (*App*) and the amyloid beta precursor-like protein 2 (*Aplp2*). Although *App* family genes are widely expressed in many types of somatic cells, the role of amyloid proteins in the inner ear is not known. The remaining γ-secretase substrates in the utricle can be divided into four classes. First, there are a number of key Notch pathway members (*Jag1*, *Jag2*, *Dner*, *Dll1*, *Notch1* and *Notch2*). Another group consists of genes involved in contact-mediated cell signaling, such as adhesion and/or neural guidance. These genes include: E- and N-cadherin (*Cdh1* and *Cdh2*), syndecans (*Sdc1, Sdc2, Sdc3*), *Robo1*, and *Ephnb1*. We also observed mRNAs for two receptor tyrosine phosphatases – *Ptprk* and *Ptprz1*. A third class consists of genes for growth factor receptors, specifically those involved in insulin-family signaling (*Igfr1* and *Insr*), as well as the EGF family receptor *Erb44*. Of the top 30 genes that code for proteins that are known substrates for γ-secretase, only three showed significant expression changes after treatment with DAPT: *Scd2* (down-regulated ~2x), and the Notch pathway members *Ser2* (increased ~2x) and *Dll1* (increased ~4x). Finally, it is notable that several of these identified γ-secretase substrates are – like Notch – also targeted by ADAM10 (e.g., App, Aplp2, N-cadherin – see Saftig and Lichtenhaler, 2015).

Discussion

Prior studies established that Notch signaling regulates the differentiation of hair cells and supporting cells during inner ear development (reviewed in Kiernan, 2013). Notch signaling is a multistep process that requires the interaction between a Notch ligand and receptor, followed by sequential proteolytic processing of the receptor by the ADAM10 metalloprotease and γ-secretase, and culminating in intercellular signaling to the nucleus and changes in gene expression (reviewed in Kopan, 2012). The present study examined the roles of ADAM10 and γ-secretase in regulating hair cell regeneration in the mature avian utricle. In agreement with prior studies conducted on other hair cell epithelia (described below), we found that inhibition of these proteases led to an increase in the numbers of replacement hair cells. Unexpectedly, we also found that inhibition of γ-secretase or ADAM10 following hair cell damage led to a significant increase in the proliferation of hair cell progenitors (supporting cells). More surprisingly, inhibition of either protease in the *undamaged* chicken utricle (which normally contains a small number of proliferating supporting cells) led to large-scale cell cycle entry among supporting cells. These results demonstrate that, in addition to controlling cell fate, γ-secretase and ADAM10 also play an essential role in the regulation of supporting cell division.

In order to help identify the molecular pathways affected by blocking these proteases, we characterized gene expression in the sensory epithelium of the utricle in response to γ-secretase inhibition. Our data indicate that inhibition of γ-secretase caused statistically significant changes in the expression levels of 253 genes. We also found that the sensory epithelium contains mRNAs for 45 proteins that are known γ-secretase substrates, including genes in the Notch signaling pathway (e.g., *Notch1* and *Dll1*). While these expression data are consistent with the hypothesis that Notch signaling regulates supporting cell division, we cannot rule out parallel contributions from other biochemical pathways that also require γ-secretase and/or ADAM10 (see below).

γ-secretase and ADAM metalloproteases regulate hair cell differentiation

Non-mammalian vertebrates have a robust ability to regenerate both auditory and vestibular hair cells following acoustic or ototoxic injury (reviewed in Warchol, 2011). In mammals, the vestibular sensory organs possess limited ability for spontaneous hair cell regeneration (e.g., Forge et al., 1993; Warchol et al., 1993; Forge et al., 1998; Kawamoto et al., 2009; Lin et al., 2011; Golub et al., 2012; Slowik et al., 2013), but lost auditory hair cells are never replaced (e.g., Forge et al., 1998). Inhibition of γ-secretase has been shown to increase hair cell differentiation during regeneration in the lateral line neuromasts of zebrafish (Ma et al., 2008), the basilar papillae of chickens (Daudet et al., 2009; Lewis et al., 2012), the utricle (Lin et al., 2011), and the organ of Corti of mice (Mizutari et al., 2013). In this study, we found that inhibition of γ-secretase with DAPT also leads to hair cell overproduction in the regenerating chicken utricle. Inhibition of ADAM10, a second protease required for Notch signaling, had a similar effect. Together, our observations of enhanced hair cell differentiation in response to Notch inhibition are consistent with these previous studies. It is also notable that the developing sensory epithelium of the mammalian cochlea contains a cellular phenotype (pillar cells) whose differentiation is not determined by Notch, but is specified by FGF signaling (Doetzlhofer et al., 2009). In our experiments, we also noted that the presumptive striolar reversal zone of the chick utricle is unaffected by inhibition of either ADAM10 or γ-secretase (e.g., Fig. 7). This observation raises the possibility that some as-yet unidentified signaling pathway (other than Notch) also regulates the phenotype of certain cells within the sensory epithelium of the utricle.

γ-secretase and ADAM metalloproteases regulate supporting cell division

In normal conditions, the vestibular organs of mature birds contain a small but measurable number of dividing supporting cells (e.g., Jørgensen and Mathiesen, 1988; Kil et al., 1997; Stone et al., 1999). Additional supporting cells are recruited to divide when hair cells are experimentally damaged, and the progeny of those divisions give rise to replacement hair cells (e.g., Weisleder and Rubel, 1993). We found that inhibition of either γ–secretase or ADAM10 caused a

significant increase in supporting cell division in chicken utricles that had been damaged with streptomycin. Notably, inhibition of either protease also caused a substantial increase in supporting cell proliferation in *undamaged* chicken utricles. It has been postulated that signals derived from hair cells normally keep supporting cells in a state of mitotic quiescence. In this model, the loss of hair cells would remove this signal, enabling supporting cells to divide and produce regenerated hair cells (reviewed in Stone and Cotanche, 2007; Warchol, 2011). Our finding that inhibition of either γ-secretase or ADAM10 causes supporting cells to divide, even when normal numbers of hair cells remain present, suggests that the transmission of this anti-proliferative signal requires activation of both γ-secretase and ADAM10. On the other hand, this notion of hair cell-mediated regulation of cell division remains hypothetical, and it is possible that γ-secretase and ADAM10 mediate a signal between supporting cells (independent of hair cells) that might also regulate cell cycle entry.

Our data also point to differences in the role of γ-secretase and notch signaling in the regulation of cell cycle entry across different inner ear sensory epithelia from differing vertebrate species. Inhibition of γ-secretase evokes proliferation of supporting cells in the cochleae of early neonatal mice (Li et al., 2015; Ni et al., 2016), and genetic deletion of *Notch1* enhances the division of progenitors in the embryonic mouse cochlea (Kiernan et al. 2005). However, inhibition of γ-secretase does not affect the proliferation of supporting cells in the mature basilar papilla of chickens, either under normal conditions or after damage (Daudet et al. 2009). Also, inhibition of γ-secretase does not stimulate regenerative proliferation in damaged utricles from adult mice (Lin et al., 2011). While these disparities cannot be explained at this time, they probably reflect fundamental differences in the mechanisms of cell cycle regulation in different sensory epithelia that may be correlated with the levels of ongoing proliferation that occur in such sensory organs. For example, unlike the chicken utricle, both the chicken basilar papilla and the mouse utricle have negligible (if any) supporting cell division in normal conditions (e.g., Corwin and Cotanche, 1988;

Yamashita and Oesterle, 1995), and very few supporting cells in the mouse utricle enter the cell cycle after hair cell damage (Kawamoto et al., 2009; Lin et al., 2011). Accordingly, supporting cell division in the chicken basilar papilla and mouse utricle is likely to be more tightly regulated than division in the chicken utricle, and abolishing this tighter regulation would require more manipulation beyond simply inhibiting γ-secretase and/or ADAM10.

Genes and pathways regulated by γ-secretase

In order to better understand how γ–secretase activity regulates supporting cell proliferation, we used RNA-seq to profile changes in gene expression in the sensory epithelium of the utricle after DAPT treatment. Some of the most robust expression changes occurred in genes involved in Notch signaling. Among those genes most strongly down-regulated by DAPT treatment were the downstream Notch effectors *Hes5* and *Heyl*, confirming that inhibition of γ-secretase caused strong reduction in Notch signaling. The expression data also point to a role for specific downstream initiators of cell cycle entry. For example, expression levels of *Ccnd3* (cyclinD3) were increased ~6-fold in response to DAPT treatment. It is of further interest to compare our data to those of a recent study that employed similar RNA-Seq methods to profile DAPT-evoked changes in gene expression in supporting cells of the mammalian cochlea at two developmental time points – P1 (a stage at which inhibition of γ-secretase leads to enhanced hair cell differentiation) and P6 (when hair cell differentiation is no longer affected by γ-secretase inhibition – Maass et al., 2016). Among the genes whose expression levels were most down-regulated by DAPT treatment, the single commonality was *Heyl*, while a comparison of the lists of the genes whose expression was most enhanced by DAPT treatment revealed no commonalities (compare Tables 1 and 2 with Tables 9 and 10 in Maass et al., 2016). These differing responses are likely to reflect differences in cellular signaling mechanisms that mediate vestibular vs. auditory phenotype as well as the early developmental stages of the treated mammalian samples.

Our RNA-Seq data also indicate that the sensory epithelium of the avian utricle expresses a number of γ-secretase substrates, the majority of which have not been studied in the context of inner ear function, development or regeneration. For example, transcripts for the amyloid precursor protein (*App*) were highly abundant, but it is not known whether *App* mRNA is translated into protein and, if so, how APP processing by γ-secretase might affect epithelial homeostasis. In addition, the utricular epithelium expresses transcripts for two receptor tyrosine phosophatases (Ptprk and Ptprz1) that are γ-secretase substrates capable of inactivating protein tyrosine kinases. Since activation of tyrosine kinases often initiates cell cycle entry, it is plausible that inhibiting γ-secretase might block the activity of PTPR's, leading to a prolonged activated state that permits ongoing cell proliferation. Although such notions are speculative, it is notable that signaling via Ptprz1 involves *both* γ-secretase and metalloproteases (Chow et al., 2008), making this phosphatase an attractive candidate for future study. The utricular macula also expresses a number of γ-secretase substrates involved in cell adhesion and contact-mediated cell guidance (e.g., *Cdh1*, *Cdh2*, *Scd2*, *Robo1*). Although N-cadherin (*Cdh2*) has been implicated in regulating the proliferation of utricular supporting cells (Warchol, 2002), we observed no change in E- or N-cadherin immunolocalization following DAPT treatment (data not shown). Finally, one limitation of our RNA-Seq studies is that they only reveal changes in gene expression, while the actual target(s) of γ-secretase and ADAM10 are almost certain to be proteins that operate upstream of transcriptional regulation.

Possible role for notch signaling in the regulation of supporting cell cycle entry

Our RNA-Seg data show that inhibition of either γ-secretase or ADAM10 resulted in a strong reduction in the expression of the notch pathway effector *Hes5*, which was correlated with a significant increase in supporting cell proliferation. RNA-Seq profiling of the regenerating chicken utricle showed that reduced expression of *Hes5* occurs immediately after ototoxic injury and prior to

the onset of regenerative proliferation (Ku et al., 2014). A similar decrease in *Hes5* transcripts also occurs in neuromasts of the zebrafish lateral line in response to hair cell injury and is followed by renewed proliferation of supporting cells (Romero-Carvajal et al. 2015). Reduced expression of *Hes5* is characteristic of an interruption in notch signaling, which may be an early injury signal in some hair cell epithelia. One working model for the chick utricle is that hair cells express ligands that interact with notch receptors on adjoining supporting cells and maintain those cells in a mitotically quiescent state. Interruption of this signal, either by the loss of hair cells or by the inhibition of γ-secretase or ADAM10, would allow supporting cells to proliferate, and cell division would continue until new hair cells have differentiated and begun to express new notch ligands. It should be emphasized that this model is speculative and would apply to cell cycle regulation in some – but not all – hair cell organs, as discussed above. Finally, our data, along with those of others (e.g., Lanford et al., 2000; Daudet et al., 2009), demonstrate that notch activity suppresses expression of the transcription factor Atoh1 during hair cell development and regeneration. Misexpression of *Atoh1* in hair cell progenitors stimulates them to divide during development (Kelly et al., 2012) and regeneration (Lewis et al., 2012). Accordingly, Atoh1 may directly or indirectly promote cell cycle entry in supporting cells after hair cell damage, and this process may be modulated by notch activity. This notion is supported by data from other tissues. For example, *Atoh1* is enriched in dividing granule cell precursors in the developing cerebellum (Ben-Arie et al., 1997), and accumulation of ATOH1 in aberrant states leads to medulloblastoma (Ayrault et al. 2010). However, ATOH1 can also serve as a tumor suppressor in other tissues, such as the colon (reviewed in Bossuyt et al., 2009).

Gene	RPKM (control)	RPKM (DAPT)	p	Fold Change (Log_2)
EDNRB2	12.65	134.95	0.03	3.4
CRB1	0.31	2.53	0.03	3.0
FSHR	0.70	4.79	0.001	2.8
LCT	1.25	8.46	0.003	2.8
CCND3	63.27	383.74	0.001	2.6
RGS5	0.38	2.03	0.003	2.4
FAM46C	2.08	10.86	0.01	2.4
PENK	8.40	41.40	0.008	2.3
MCM6	26.14	126.17	0.005	2.3
CDCA7	6.36	30.27	0.006	2.3
WNT16	0.12	0.57	0.04	2.2
UNG	10.84	45.58	0.009	2.1
FOXN4	1.54	6.47	0.002	2.1
TMEM116	1.27	5.29	0.02	2.1
EMID1	0.97	3.92	0.003	2.0
MYCL1	14.48	57.73	0.001	2.0
MCM5	31.47	124.0	0.008	2.0
E2F1	18.17	71.44	0.02	2.0
FTL	42.64	164.55	0.005	1.9
MYBL1	2.53	9.59	0.02	1.9
NXPH3	4.40	16.55	0.02	1.8
GPR144	2.42	9.06	0.001	1.9
DLL1	29.54	110.52	0.02	1.9
CYP2C18	0.54	1.99	0.02	1.9
SLBP	2.74	9.78	0.02	1.8

Table 1. List of 25 gene transcripts that displayed the largest increases in expression in response to DAPT treatment, relative to controls. Mean abundance levels for each gene are normalized values and are expressed as ‘reads per kilobase per million mapped reads’ (RPKM).

Gene	RPKM (control)	RPKM (DAPT)	p	Fold Change (Log_2)
HES5	213.22	14.91	0.001	-3.8
GCNT3	1.13	0.19	0.02	-2.6
EGF	5.14	1.11	0.03	-2.2
TSGA14	118.32	26.31	0.001	-2.2
HEYL	92.82	20.70	0.009	-2.2
KCTD4	2.05	0.49	0.001	-2.1
FSHB	1.27	0.36	0.02	-1.8
HEBP2	3.30	0.95	0.02	-1.8
MLC1	22.53	6.55	0.01	-1.8
GCHFR	51.84	15.17	0.01	-1.8
CNTN4	0.68	0.22	0.01	-1.7
FOXD3	3.40	1.12	0.01	-1.6
A2M	91.69	31.22	0.008	-1.6
JAKMIP1	0.52	0.19	0.05	-1.5
JAG1	182.63	66.44	0.04	-1.5
F3	342.87	128.50	0.02	-1.4
SUSD5	1.09	0.42	0.01	-1.4
LMO3	12.01	4.66	0.03	-1.4
WNT7A	32.60	12.67	0.02	-1.4
NOG	3.22	1.27	0.007	-1.3
ATP12A	3.15	1.24	0.04	-1.3
WFIKKN1	0.59	0.23	0.01	-1.3
TMSB10	1.78	0.72	0.03	-1.3
C13Horf4	4.80	1.97	0.03	-1.3
GJB6	329.80	136.64	0.03	-1.3

Table 2. List of 25 gene transcripts that showed the largest decreases in expression in response to DAPT treatment, relative to controls. Reads for each gene are normalized values and are expressed as ‘‘reads per kilobase per million mapped reads’ (RPKM).

Gene	RPKM
APP	1275.79
APLP2	1066.8
CDH1	253.943
EPCAM	242.758
JAG1	182.628
SDC2	163.658
CDH2	130.781
PTPRK	125.611
SDC1	104.647
DNER	82.7559
PTPRZ1	73.7772
IGF1R	57.668
NOTCH1	54.2543
EFNB1	48.7694
CD44	41.3677
ROBO1	39.683
NOTCH2	38.4623
SDC3	37.6648
JAG2	36.2181
ERBB4	34.712
PLXDC2	32.194
DLL1	29.5427
INSR	28.2952
PAM	26.2218
SORCS1	20.3676

Table 3. List of 25 most-abundant transcripts encoding γ-secretase substrates that are present (but not necessarily differentially expressed) in the utricular sensory epithelium. Reads for each gene are normalized values and are expressed as 'reads per kilobase per million mapped reads' (RPKM).

References

Bai G, Pfaff SL (2011) Protease regulation: the Yin and Yang of neural development and disease. Neuron 72: 9-21.

Chuang CH, Yang D, Bai G, Freeland A, Pruit SC, Schimenti JC (2012) Post-transcriptional homeostasis and regulation of MCM2-7 in mammalian cells. Nucleic Acids Res 40: 4914-4924.

Corwin JT, Cotanche DA (1988) Regeneration of sensory hair cells after acoustic trauma. Science 240: 1772-1774.

Daudet N, Gibson R, Shang J, Bernard A, Lewis J, Stone J (2009) Notch regulation of progenitor cell behavior in quiescent and regenerating auditory epithelium of mature birds. Dev Biol 326: 86-100.

Demehri S, Turkoz A, Kopan R (2009) Epidermal Notch1 loss promotes skin tumorigenesis by impacting the stromal microenvironemnt. Cancer Cell 16: 55-66.

Doetzlhofer A, Basch ML, Ohyama T, Gessler M, Groves AK, Segil N (2009) Hey2 regulation by FGF provides a Notch-independent mechanism for maintaining pillar cell fate in the organ of Corti. Dev Cell 16: 58-69.

Forge A, Li L, Corwin JT, Nevill G. (1993) Ultrastructural evidence for hair cell regeneration in the mammalian inner ear. Science. 259:1616-9.

Forge A, Li L, Nevill G. (1998) Hair cell recovery in the vestibular sensory epithelia of mature guinea pigs. J Comp Neurol. 397:69-88.

Golub TS, Tong L, Ngyuen TB, Hume CR, Palmiter RD, Rubel EW, Stone JS. (2012) Hair cell replacement in adult mouse utricles after targeted ablation of hair cells with diphtheria toxin. J Neurosci 32: 15093-15105.

Haapasalo A, Kovacs DM (2011) The many substrates of presenilin/[redacted]secretase. J Alzheimers Dis 25: 3-28.

Haddon C, Jiang YJ, Smithers L, Lewis J (1998) Detah-Notch signaling and the patterning of sensory cell differentiation in the zebrafish ear: evidence from the mind bomb mutant. Development 125: 4637-4644.

Harris ML, Hall R, Erikson CA (2008) Directing pathfinding along the dorsolateral path – the role of EDNRB2 and EphB2 in overcoming inhibition. Development 135: 4113-4122.

Hartman BH, Nelson BR, Reh TA, Bermingham-McDonogh O (2010) Delta/notch EGF-related receptor (DNER) is expressed in hair cells and neurons

in the developing and adult mouse inner ear. J Assoc Res Otolaryngol 11: 187-201.

Henrique D, Adam J, Myat A, Chitnis A, Lewis J, Ish-Horowicz D (1995) Expression of a Delta homologue in prospective neurons in the chick. Nature 375: 787-790.

Hundhausen C, Misztela D, Berkhout TA, Broadway N, Saftig P, Reiss K, Hartmann D, Fahrenholtz F, Postina R, Matthews V, Kallen KJ, Rose-John S, Ludwig A (2003) The disintegrin-like metalloproteinase ADAM10 is involved in constitutive cleavage of CX3CL1 (fractalkine) and regulates CX3CL1-mediated cell-cell adhesion. Blood 102: 1186-1195.

Jørgensen, J.M. and Mathiesen, C. (1988) The avian inner ear: continuous production of hair cells in vestibular sensory organs, but not in the auditory papilla. Naturwissenschaftern 75: 319-320.

Jørgensen, J.M. (1989) Number and distribution of hair cells in the utricular macula of some avian species. J Morphol 201: 187-204.

Kawamoto K, Izumikawa M, Beyer LA, Atkin GM, Raphael Y (2009) Spontaneous hair cell regeneration in the mouse utricle following gentamicin ototoxicity. Hearing Res 247: 17-26.

Kelley MW (2006) Regulation of cell fate in the sensory epithelia of the inner ear. Nat Rev Neurosci 7: 837-849.

Kiernan AE, Cordes R, Kopan R, Gossler A, Gridley T (2005) The Notch ligands DLL1 and JAG2 act synergistically to regulate hair cell development in the mammalian inner ear. Development 132: 4353-4362.

Kiernan AE (2013) Notch signaling during cell fate determination in the inner ear. Semin Cell Dev Biol 24: 470-479.

Kil J, Warchol ME, Corwin JT. (1997) Cell death, cell proliferation, and estimates of hair cell life spans in the vestibular organs of chicks. Hearing Res. 144: 117-126

Kopan R, Ilagan MX (2009) The canonical Notch signaling pathway: unfolding the activation mechanism. Cell 137: 216-233.

Kopan R (2012) Notch signaling. Cold Spring Harbor Perspectives in Biology. 4: a011213.

Korvatska O, Estes A, Munson J, Dawson G, Bekris LM, Kohen R, Yu CE, Schellenberg GD, Raskind WH (2011) Mutations in the TSGA14 gene in families

with autism spectrum disorders. Am J Med Genet B Neuropsych Genet 156B: 303-311.

Ku YC, Renaud NA, Veilie RA, Helms C, Voelker CC, Warchol ME, Lovett M (2014) The transcriptome of utricle hair cell regeneration in the avian inner ear. J Neurosci 34: 3523-3535.

Lanford PJ, Lan Y, Jiang R, Lindsell C, Weinmaster C, Gridley T, Kelley MW (1999) Notch signaling pathway mediates hair cell development in mammalian cochlea. Nat Genet 21: 289-292.

Lewis RM, Hume CR, Stone JS (2012) Atoh1 expression and function during auditory hair cell regeneration in post-hatch chickens. Hearing Res 289: 74-85.

Li W, Wu J, Yang J, Sun S, Chai R, Chen ZY, Li H (2015) Notch inhibition induces mitotically generated hair cells in mammalian cochleae via activating the Wnt pathway. Proc Natl Acad Sci USA 112: 166-171.

Lin V, Golub JS, Nguyen TB, Hume CR, Oesterle EC, Stone JS (2011) Inhibition of Notch activity promotes nonmitotic regeneration of hair cells in the adult mouse utricle. J Neurosci 31: 15329-15339.

Lopez I, Ishiyama G, Tang Y, Tokita J, Baloh RW, Ishiyama A. (2005) Regional estimates of hair cells and supporting cells in the human crista ampullaris. J Neurosci Res 82(3):421-31

Ma EY, Rubel EW, Raible DW (2008) Notch signaling regulates the extent of hair cell regeneration in the zebrafish lateral line. J Neurosci. 28:2261-73.

Maass JC, Gu R, Cai T, Wan YW, Cantellano SC, Asprer JST, Zhang H, Jen HI Edlund RK, Liu Z, Groves AK (2016) Transcriptomic analysis of mouse cochlear supporting cell maturation reveals large-scale changes in Notch responsiveness prior to the onset of hearing. PLoS One 11: e0167286.

Merchant SN, Velazquez-Villaseñor L, Tsuji K, Glynn RJ, Wall C 3rd, Rauch SD (2000) Ann Otol Rhinol Laryngol Suppl 181:3-13.

Mizutari K, Fujioka M, Hosoya M, Bramhall N, Okano HJ, Edge AS (2013) Notch inhibition induces cochlear hair cell regeneration and recovery of hearing after acoustic trauma. Neuron 77: 58-69.

Ni W, Lin C, Wu J, Chen Y, Chai R, Li W, Ki H (2016) Extensive supporting cell proliferation and mitotic hair cell generation by in vivo genetic reprogramming in the neonatal mouse cochlea. J Neurosci 36: 8734-8745.

Pfaffl MW (2001) A new mathematical model for relative quantification in real-time RT-PCR. Nucleic Acids Res 29: e45.

Park JC, Hubel SB, Woods AD (1987) Morphometric analysis and fine structure of the vestibular epithelium of aged C57BL/6NNia mice. Hear Res. 28: 87-96.

Raft S, Groves AK (2014) Segregating neural and mechanosensory fates in the developing ear: patterning, signaling, and transcriptional control. Cell Tissue Res DOI 10.1007/s00441-014-1917-1926

Rauch SD, Velazquez-Villaseñor L, Dimitri PS, Merchant SN (2001) Decreasing hair cell counts in aging humans. Ann N Y Acad Sci. 220-7.

Roberson DF, Weisleder P, Bohrer PS, Rubel EW (1992) Ongoing production of sensory cells in the vestibular epithelium of the chick. Hearing Res 57: 166-174.

Saftig P, Lichtenthaler SF (2015) The alpha secretase ADAM10: A metalloprotease with multiple functions in the brain. Prog Neurobiol 135: 1-20.

Sankaran VG, Ludwig LS, Sicinska E, Xu J, Bauer DE, Eng LC, Patterson HC, Metcalf RA, Natkunam Y, Orkin SH, Sicinski P, Lander ES, Lodish HF (2012) Cyclin D3 coordinates the cell cycle during differentiation to regulate erythrocyte size and number. Gens Dev 26: 2075-2087.

Sienknecht UJ, Fekete DM (2008) Comprehensive Wnt-related gene expression during cochlear duct development in chicken. J Comp Neurol 510: 378-395.

Stenman JM, Rajagopal J, Carroll TJ, Ishibashi M, McMahon J, McMahon AP (2008) Canonical Wnt signaling regulates organ-specific assembly and differentiation of CNS vasculature. Science 322: 1247-1250.

Stone JS, Rubel EW (1999) Delta1 expression during avian hair cell regeneration. Development 126: 961-973.

Stone JS, Cotanche DA. (2007) Hair cell regeneration in the avian auditory epithelium. Int J Dev Biol. 51:633-47.

Stone JS, Choi YS, Woolley SM, Yamashita H, Rubel EW. (1999) Progenitor cell cycling during hair cell regeneration in the vestibular and auditory epithelia of the chick. J Neurocytol. 28:863-76.

Trapnell C, Pachter L, Salzberg SL (2009) TopHat: discovering splice junctions with RNA-Seq. Bioinformatics 25:1105-1111.

van Tetering G, van Diest P, Verlaan I, van der Wall E, Vooijs M (2009) Metalloprotease ADAM10 is required for Notch1 site 2 cleavage. J Biol Chem 284: 31018-31027.

Warchol ME (2002) Cell density and N-cadherin interactions regulate cell proliferation in the sensory epithelia of the inner ear. J Neurosci 22: 2607-2616.

Warchol ME, Montcouquiol M (2010) Maintained expression of the planar cell polarity molecule Vangl2 and reformation of hair cell orientation in the regenerating inner ear. J Assoc Res Otolaryngol 11: 395-406.

Warchol ME (2011) Sensory regeneration in the vertebrate inner ear: Differences at the levels of cells and species. Hearing Res 273: 72-79.

Weisleder P, Rubel EW (1993) Hair cell regeneration after streptomycin toxicity in the avian vestibular epithelium. J Comp Neurol 331: 97-110.

Yamashita H, Oesterle EC (1995) Induction of cell proliferation in mammalian inner-ear sensory epithelia by transforming growth factor-α and epidermal growth factor. Proc Natl Acad Sci USA 92: 3152-3155.

Figure Legends

Figure 1. Inhibition of γ-secretase or ADAM10 in the regenerating utricle leads to increased numbers of replacement hair cells. Utricles were placed in organotypic culture and hair cells were killed by treatment for 24 hr with 1 mM streptomycin. Specimens were then rinsed and allowed to recover for 7 d. During this period, some regenerating utricles were treated with 10 μM DAPT (an inhibitor of γ-secretase), 10 μM GI254023X (a specific inhibitor of ADAM10), or 0.1% DMSO (controls). After fixation, hair cells were identified via immunoreactivity for myosin VIIa (red) and filamentous actin was labeled with phalloidin (green). Utricles that were treated with DAPT or GI254023X contained enhanced numbers of hair cells, compared to controls. This increase was particularly notable in the striolar region (middle column). Scale bar = 50 μm.

Figure 2. Inhibition of γ-secretase increases regenerative proliferation in the chicken utricle. Cultured utricles were treated for 24 hr with 1 mM streptomycin and then rinsed and maintained for 48 hr in either 10 μM DAPT or 0.1% DMSO (controls). Proliferating cells were identified by addition of the mitotic tracer BrdU to the culture medium for the final 4 hr *in vitro*. Although numerous proliferating cells were observed in untreated (control) specimens (A), many more BrdU-labeled cells were observed in the DAPT-treated utricles (B). Quantification of BrdU-labeled cells indicates that DAPT treatment enhanced regenerative proliferation by ~3-fold. Data were compiled from three independent experiments of 3-4 utricles/condition, yielding a total of 10-12 utricles/group. Plot shows mean±SD. Scale bar = 60 μm.

Figure 3. Inhibition of γ-secretase evokes cell cycle entry in undamaged utricles. Cultured utricles were treated for 48 hr with 10 μM DAPT or 0.1% DMSO (controls). Proliferative cells were labeled by the addition of BrdU to the medium for the final four hours of culture. Although some BrdU-labeled cells were observed in control utricles (A), treatment for 48 hr with DAPT resulted in many additional BrdU-labeled cells (B, C). Data were compiled from three

independent experiments of 3-4 utricles/condition, yielding a total of 10-12 utricles/group. Plot shows mean±SD. (D) Double-labeling for BrdU (green) and myosin VIIa (red) suggests that BrdU-labeled nuclei are not associated with myosin VIIa-labeled cell bodies, indicating that such proliferating cells are supporting cells. Scale bars: (B) 60 μm; (D) 30 μm.

Figure 4. Inhibition of metalloproteases promotes cell cycle entry in undamaged utricles. Utricles were placed in culture and treated for 48 hr in either 0.1% DMSO (control), GM6001 (20 μM; a broad spectrum inhibitor of matrix metalloproteases), TAPI-2 (50 μM, an inhibitor of TACE-family metalloproteases), or GI254023X (10 μM; a specific inhibitor of ADAM10). Proliferating cells were labeled by addition of BrdU to the medium for the final 4 hr *in vitro*. Treatment with all inhibitors resulted in increased proliferation, relative to control specimens. Data were compiled from three independent experiments of 3-4 utricles/condition, yielding a total of 10-12 utricles/group. Plot shows mean±SD. Scale bar = 30 μm.

Figure 5. Inhibition of γ-secretase or ADAM10 does not cause hair cell death. Utricles were placed in culture and maintained for 48 hr in either 10 μM DAPT (top), 10 μM GI254023X (middle), or 0.1% DMSO (bottom, control). Specimens were then fixed and immunolabeled for otoferlin (HCS-1), in order to identify hair cells. Quantification of labeled hair cells (green) revealed nearly identical densities in all specimens. This observation indicates that neither DAPT nor GI254023X directly damages hair cells and suggests that the proliferative effect of these inhibitors (e.g., Fig. 4) is not a secondary consequence of hair cell injury. Data were compiled from 3 independent experiments of 3-4 utricles/condition, yielding a total of 10-12 utricles/group. Plot shows mean±SD. Scale bar = 10 μm.

Figure 6. Inhibition of γ-secretase leads to enhanced proliferation in cultures of isolated utricular sensory epithelia. Explanted utricles were

treated for 1 hr in thermolysin and intact sensory epithelia were then isolated and plated onto laminin-coated glass substrates. After 2-3 days *in vitro*, specimens were treated with either 10 μM DAPT or 0.1% DMSO, and maintained in culture for an additional 24 hr. Proliferating cells were labeled by addition of BrdU to the medium for the final 4 hr. Imaging of BrdU-labeled cells (green) revealed many more proliferating cells in DAPT-treated cultures (top) than in controls (middle). Quantification of BrdU-labeled cells confirmed this observation ($p<0.005$). This result indicates that the proliferative response of cells in the sensory epithelia of the utricle does not require signaling from the underlying stromal tissue. Data were compiled from three independent experiments of 3-4 isolated epithelia/condition, yielding a total of 10-12 epithelia/group. Plot shows mean$\pm$SD. Blue label=DAPI. Scale bar=30 μm.

Figure 7. The presumed reversal zone of the striola does not respond to γ-secretase inhibition. (A) Schematic diagram of the chick utricle showing the location of the striola. The reversal zone is a region of 8-10 cell widths that runs through the center of the striola. (B) Treatment for 48 hr in 10 μM DAPT evoked high levels of cell proliferation throughout the sensory region of the utricle, *except* for the striolar reversal zone (arrows). Images C-E' show a portion of striolar region that is indicated by the red square in (A). (C, C') High magnification views demonstrating the large increase in proliferation in response DAPT treatment (C') except for the reversal zone (arrowhead, C'). (D, D') DAPT treatment also resulted in increased numbers of myosin VIIa-labeled cells hair cells in all regions of the utricle *except* the central zone (arrowhead, D') (E, E') DAPT treatment caused a reduction in the spatial domain of β-tectorin expression (arrowheads, E'). Scale bar = 10 μm.

Figure 8. γ-secretase inhibition resulted in increased numbers of ATOH1-expressing cells, some of which were mitotically active. Cultured utricles were treated for 24 hr with 100 μM streptomycin and were then maintained for 24 hr in streptomycin-free media that contained either: (A) 0.1% DMSO or (B) 10 μM

DAPT. The mitotic tracer BrdU was added to media for the final 4 hr *in vitro*. DAPT treatment led to enhanced numbers of both ATOH1-labeled (red) and BrdU-labeled (green) nuclei, compared to controls (B vs. A). Some cells were double-labeled for both ATOH1 and BrdU (arrowheads). Cultures that were treated with DAPT for 6 days also contained numerous BrdU-labeled hair cells (C, arrows).

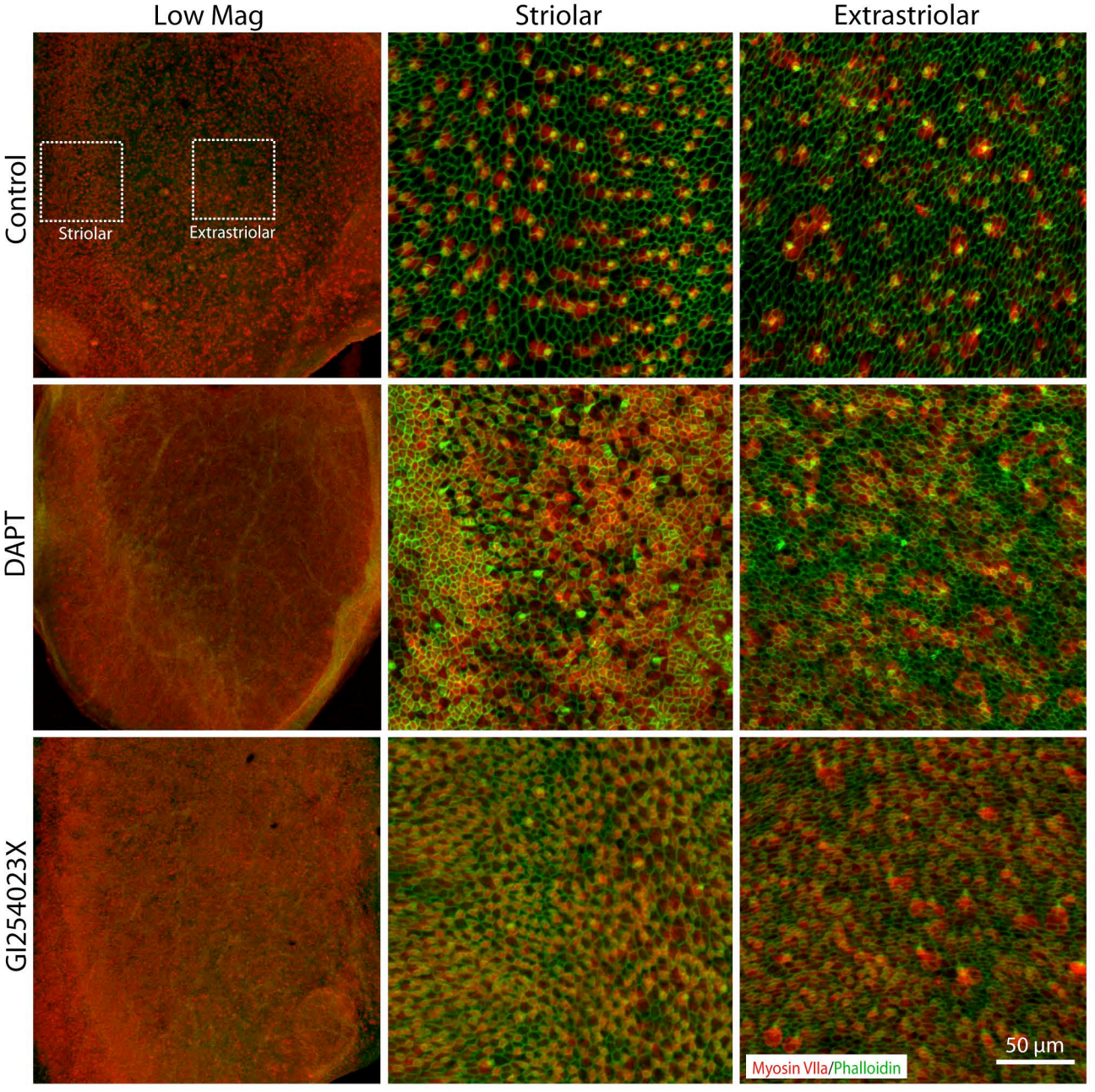
Low Mag
Striolar
Extrastriolar
Control
DAPT
GI254023X
Striolar
Extrastriolar
50 µm
Myosin VIIa/Phalloidin

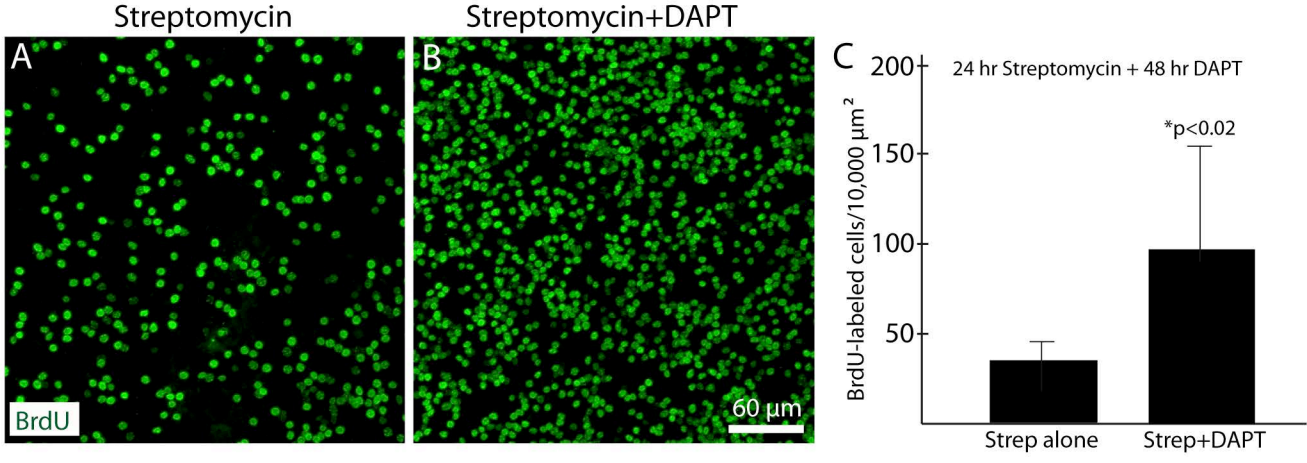
Streptomycin
Streptomycin+DAPT
A
B
BrdU
60 µm
C
24 hr Streptomycin + 48 hr DAPT
*p<0.02
BrdU-labeled cells/10,000 µm²
200
150
100
50
Strep alone
Strep+DAPT

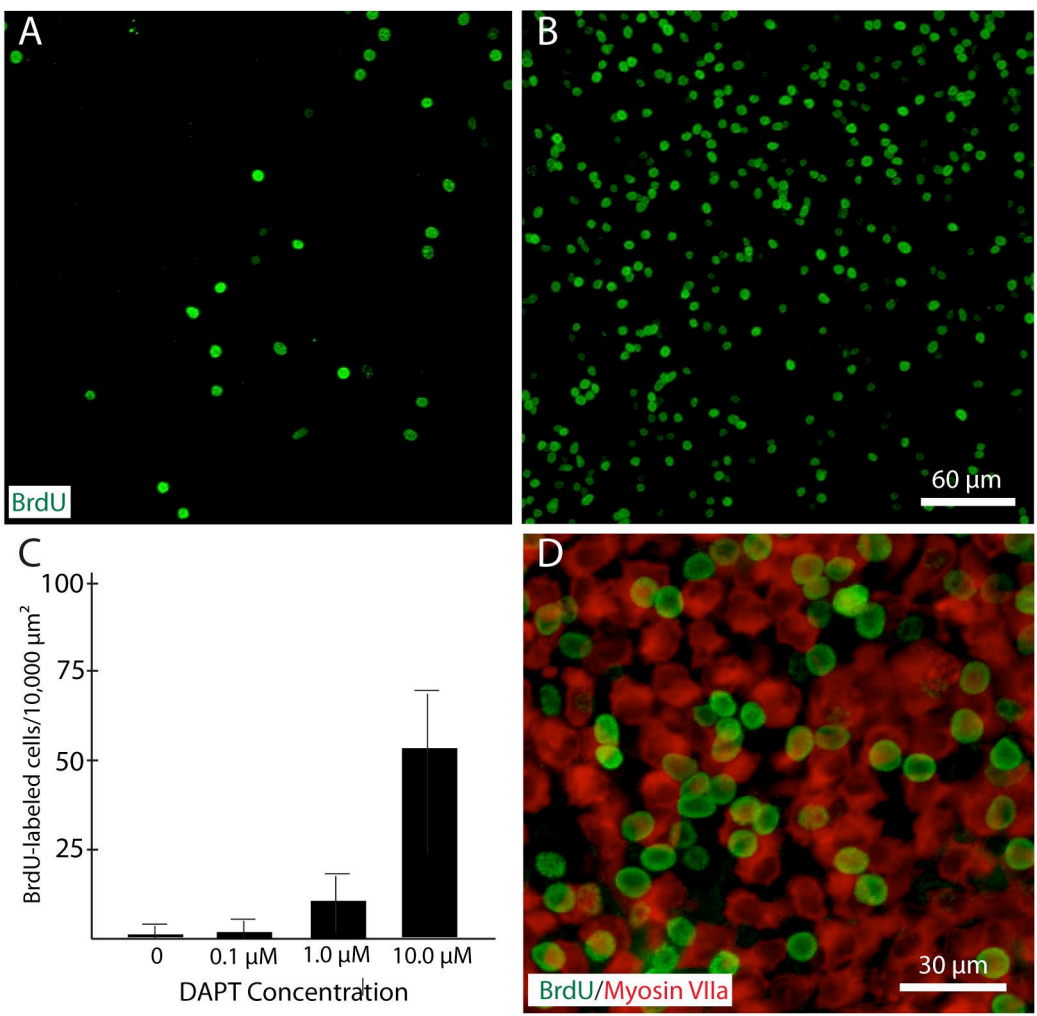
A
BrdU
B
60 µm
C
100
75
50
25
BrdU-labeled cells/10,000 µm²
0
0.1 µM
1.0 µM
10.0 µM
DAPT Concentration
D
BrdU/Myosin VIIa
30 µm

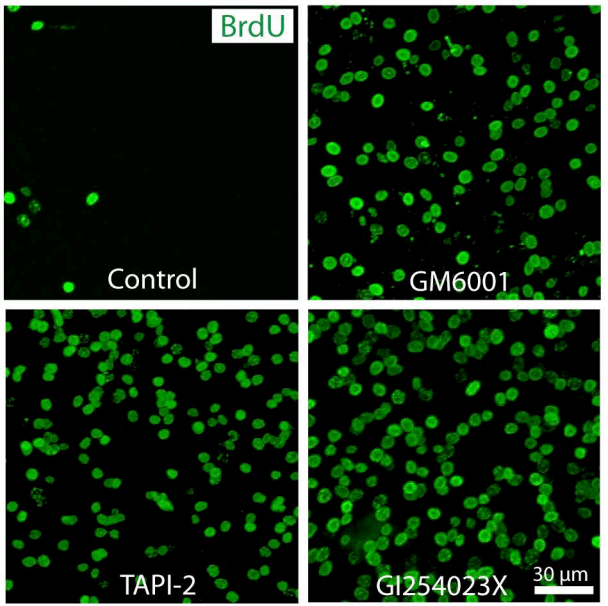
BrdU
Control
GM6001
TAPI-2
GI254023X
30 µm

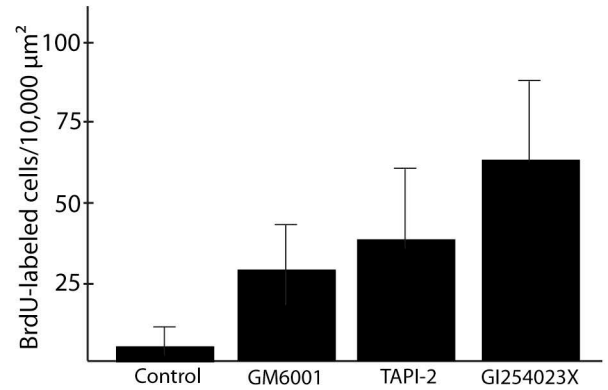
BrdU-labeled cells/10,000 µm²
100
75
50
25
Control
GM6001
TAPI-2
GI254023X

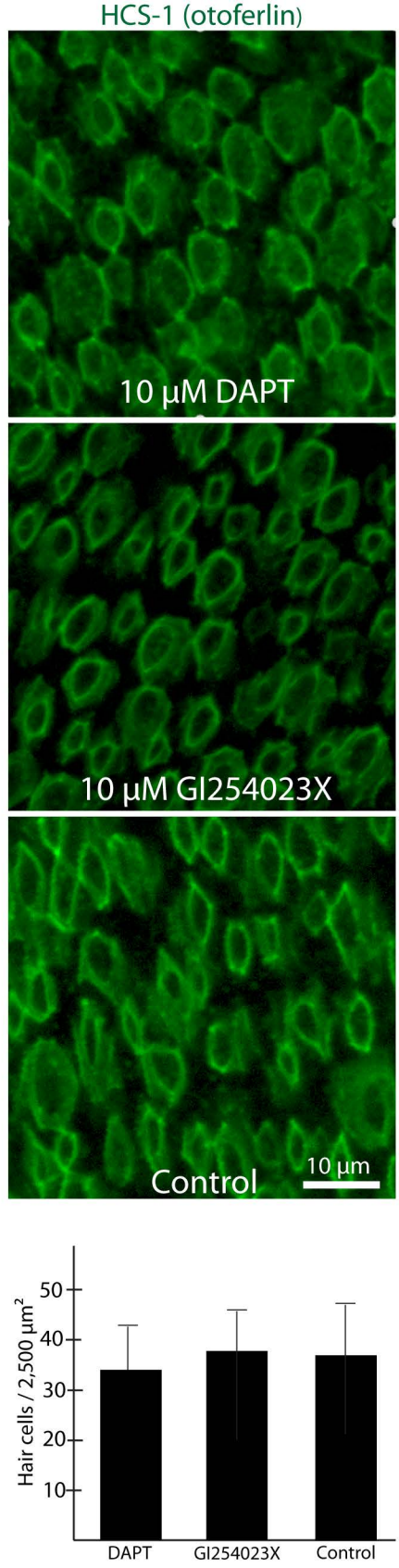
HCS-1 (otoferlin)
10 µM DAPT
10 µM GI254023X
Control
10 µm
Hair cells / 2,500 µm²
50
40
30
20
10
DAPT
GI254023X
Control

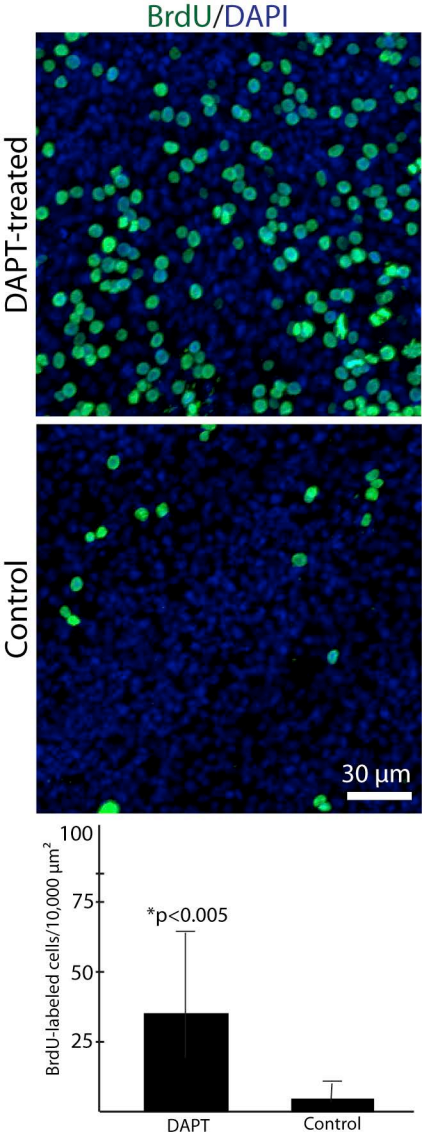
BrdU/DAPI
DAPT-treated
Control
30 µm
BrdU-labeled cells/10,000 µm²
100
75
50
25
*p<0.005
DAPT
Control

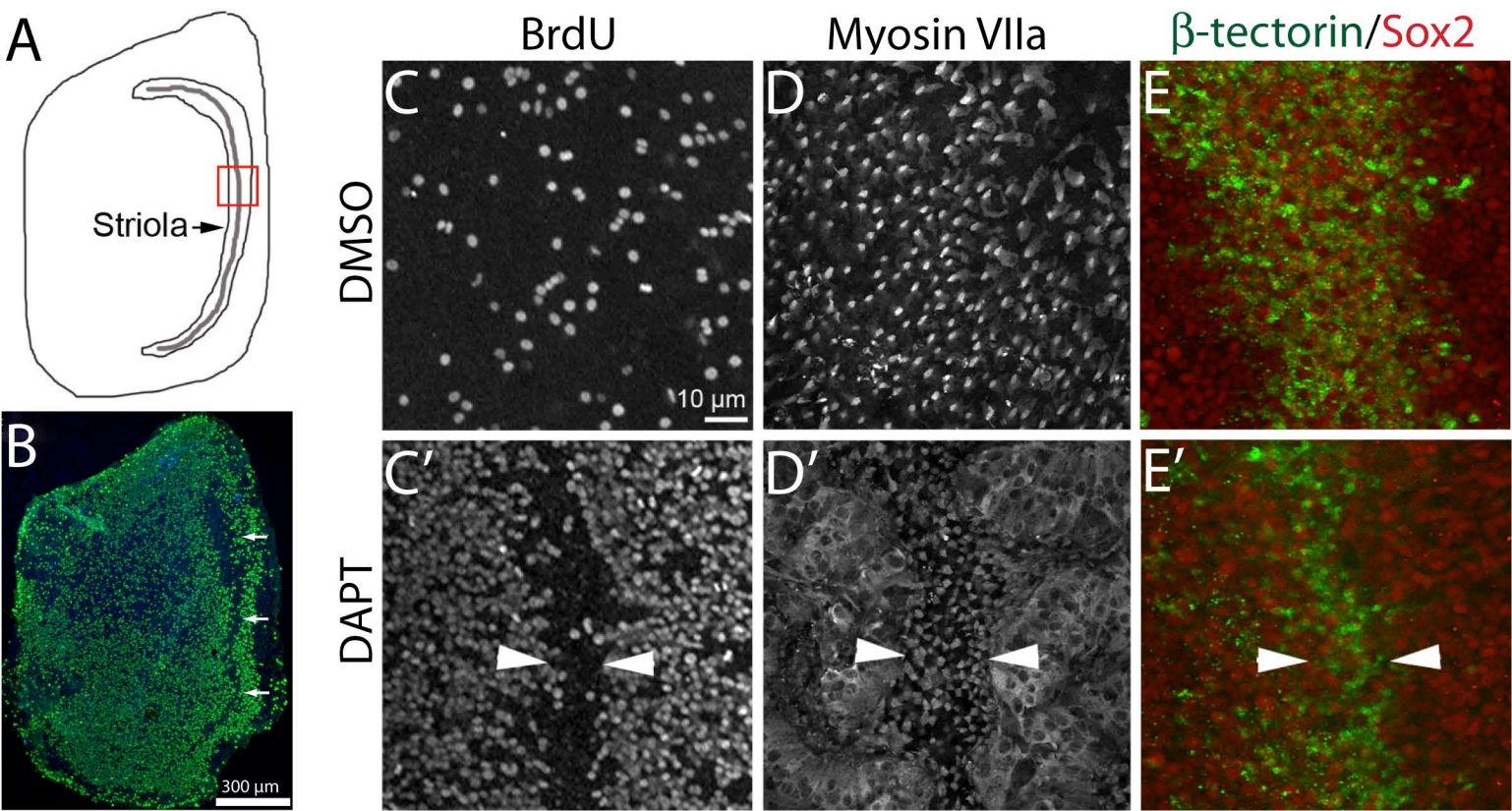
A
Striola
B
300 μm
BrdU
Myosin VIIa
β-tectorin/Sox2
DMSO
DAPT
C
D
E
C′
D′
E′
10 μm

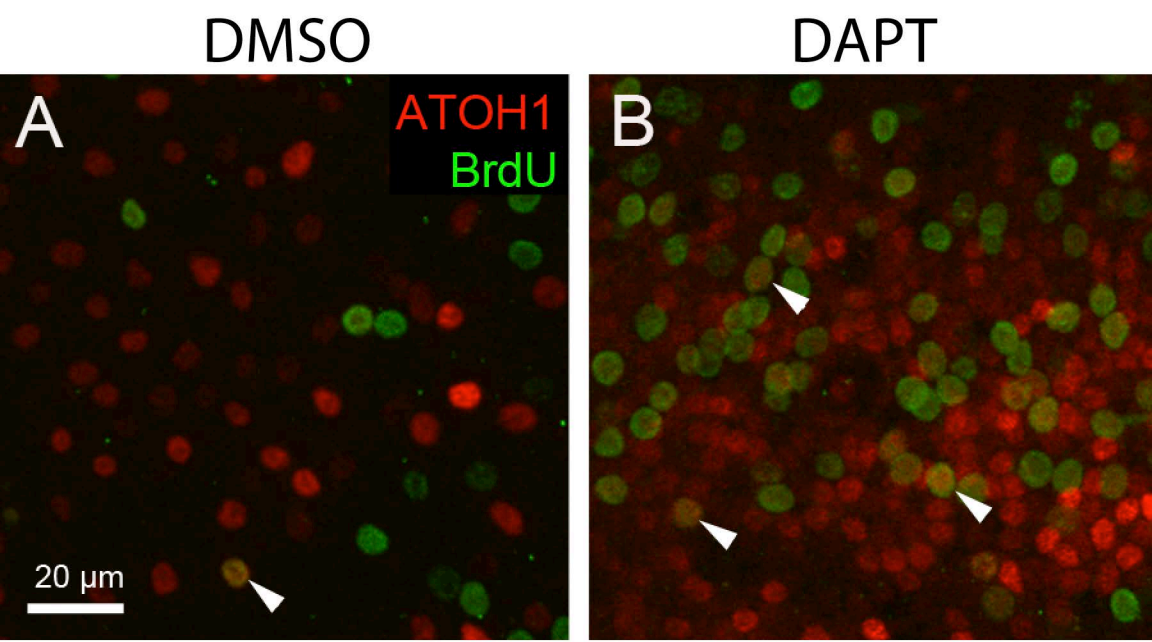
DMSO
DAPT
A
B
ATOH1
BrdU
20 μm